Received: 2 February 2022 | Revised: 21 March 2022 | Accepted: 22 April 2022

DOI: 10.1002/eqe.3662

RESEARCH ARTICLE

WILEY

Kinematic response of vertical and batter pile groups in non-linear soft soil

Miran Cemalovic[1,2] | **Jan B. Husebø**[1,3] | **Amir M. Kaynia**[2,4]

[1]Structural Engineering Technology, Sweco Norway AS, Bergen, Norway

[2]Department of Structural Engineering, Norwegian University of Science and Technology, Trondheim, Norway

[3]Department of Civil Engineering, Western Norway University of Applied Sciences, Bergen, Norway

[4]Geotechnics, Norconsult AS, Sandvika, Norway

Correspondence
Miran Cemalovic, Fantoftvegen 14P, 5072 Bergen, Norway.
Email: miran.cemalovic@sweco.no

Present address
Fantoftvegen 14P, 5072 Bergen, Norway

Funding information
Sweco Norway AS; Norges Forskningsråd

Abstract

This paper presents a comprehensive numerical study on kinematic response of vertical and batter pile groups in soft soil, where soil non-linearity, batter angle, pile spacing and excitation frequency are related to pile-cap displacements, rotations, maximum pile moments, shear forces and axial forces. The finite element model is constructed in OpenSees MP, and parallel computing is utilized for a better (faster) performance. Results reveal that soil non-linearity has a profound impact on the kinematic interaction. Increasing batter angle decreases horizontal displacements but increases rotations. Batter pile groups yield lower spectral accelerations compared to vertical pile groups. For high *PGA*, the spectral accelerations of the pile-cap may be lower compared to the spectral acceleration of the seismic input motion. Estimation using non-linear interaction factors conservatively estimates pile-cap displacements and rotations, while roughly captures the effects with respect to batter angle and frequency content within the specified framework.

KEYWORDS
batter piles, clay, kinematic interaction, non-linear, numerical

1 | INTRODUCTION

Until the early 1990s, batter piles were commonly used in seismic design of bridges and other large structures. In the following years however, batter piles became generally discouraged due to several earthquakes where batter piles experienced severe damage. As of today, numerous governing codes, including Eurocode 8,[1] recommend that batter piles are avoided in seismic design of deep foundations. The advancement in computational methods during the last two decades has facilitated numerous numerical studies that spurred on a more positive outlook on the use of batter piles in seismic design. Sadek and Isam[2] showed that batter micro-piles lead to a decrease in both shear force and bending moment induced by seismic loading. Gerolymos and Giannakou[3] concluded that batter piles with hinged pile-to-cap connections performed better than vertical piles when supporting tall, slender structures. Giannakou et al.[4] concluded along the same lines, emphasizing that vertical piles attracted larger axial forces when supporting tall structures. Medina et al.[5] explored how batter pile groups influence the overall response of slender and non-slender structures using a substructure approach. It was shown that batter piles reduce pile-cap displacements and base shear forces for non-slender structures. Carbonari et al.[6] investigated the seismic response of bridge piers on batter pile groups using a direct approach in the frequency

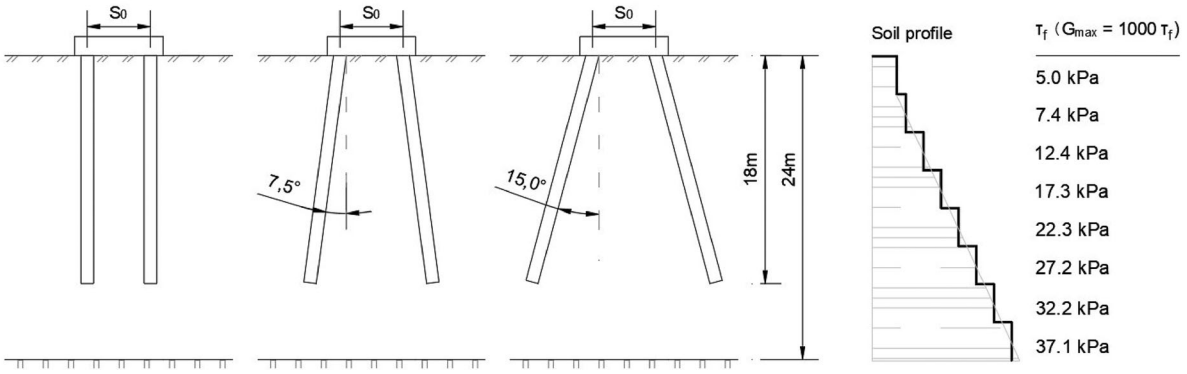

FIGURE 1 Schematic sketch of the investigated pile–soil system

domain. It was demonstrated that batter piles reduce pile-cap displacements but increase rotations. A few experimental studies revealed similar advantages. Escoffier[7] performed an experimental study elucidating frequency-dependent behaviour of a two-by-one pile group. It was shown that batter piles reduce pile-cap displacements. Subramanian et al.[8] found that the lateral displacement and bending strain at resonance region decrease with increasing batter angle for a two-by-one pile group subjected to lateral loads. Bharathi et al.[9] found that peak displacements of batter pile groups were significantly reduced compared to vertical pile groups.

Extensive studies have been performed on kinematic interaction of vertical piles using linear models,[10–22] but substantially less attention has been paid to batter piles. Medina et al.[23] presented a comprehensive linear method based on a BEM-FEM coupled formulation for estimating kinematic interaction of batter pile groups. Dezi et al.[24] presented a numerical model for dynamic analysis of batter pile groups in layered soil. Carbonari et al.[25] presented an analytical, closed-form solution for dynamic stiffness and kinematic response of single batter piles. Indeed, a few authors have carried out non-linear studies using vertical and batter piles,[26–30] but kinematic interaction of batter pile groups in non-linear soil has yet to be investigated.

Kinematic interaction is most prominent in soft soils, and several researchers[4,12,22] have elucidated the importance of soil profile on kinematic interaction of pile groups. This paper focuses, therefore, on the kinematic response of vertical and batter pile groups in soft clay using a simplified, yet realistic clay profile. Further details regarding the soil are given in Section 2.2. The investigated system is the two-by-one pile group depicted in Figure 1, which is representative of a bridge abutment or pier foundation. The total profile height H is 24 m, the pile length l_p is 18 m and the pile diameter d_p is 1 m. This study considers three different pile-to-pile spacings S_0 equal to $2d_p$, $6d_p$ and $10d_p$ together with three different batter angles β equal to 0°, 7.5° and 15°, all of which are considered to be within realistic range of values.

Vertically propagating seismic S-waves cause horizontal displacement of the free-field soil. Rigid structures such as pile foundations tend to resist the free-field motion, generating modified displacements and rotations of the pile-cap. The relationship between the free-field and pile-cap motion is often expressed through horizontal and rotational kinematic interaction factors,

$$I_x = \frac{U_p(\omega)}{U_f(\omega)}, \quad I_r = \frac{\phi_p(\omega)\, d_p}{U_f(\omega)} \tag{1}$$

where U_p is the horizontal pile-cap displacement amplitude, U_f is the horizontal free-field displacement amplitude, ϕ_p is the pile-cap rotation and ω is the angular frequency. Note that the literature occasionally presents I_r as a function of S_0 instead of d_p. The nomenclature in this paper is motivated by the desire to clearly express how rotation varies with pile spacing. In the rather convenient realm of linearity, the kinematic interaction factors may readily be applied in the substructure method by multiplying the free-field motion in the frequency domain with the corresponding interaction factor. Since this procedure implies superposition, interaction factors lack the practical applicability in non-linear analysis in the most rigorous sense. Nevertheless, non-linear interaction factors provide useful information about kinematic response of pile groups. First, frequency-dependent modification of the free-field motion is readily depicted. Second, linear and non-linear interaction factors are directly comparable, providing insight into differences in kinematic pile–soil interaction between linear and non-linear models. Perhaps somewhat obvious, it is worth mentioning that interaction factors presented in the frequency domain equivalently provide information about differences in pile-cap accelerations.

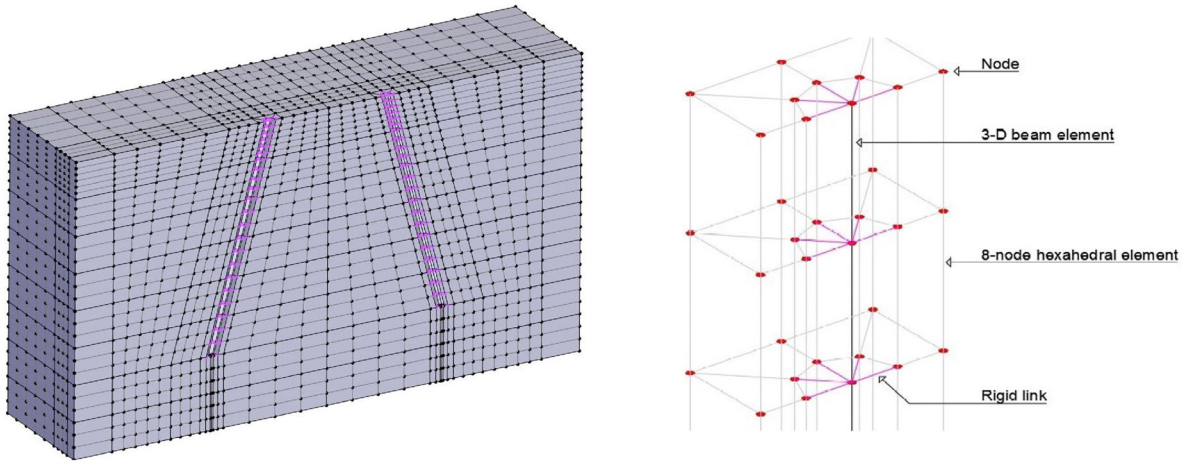

FIGURE 2 Three-dimensional finite element model

The main objective of this paper is to provide further insight into how non-linearity, batter angle, pile spacing and excitation frequency affect pile-cap displacements, rotations, maximum pile moments, shear forces and axial forces. First, the finite element model and the adopted soil model are outlined. Next, the results from harmonic base motion analyses are presented and discussed. We further extend the analyses to time domain and discuss the findings in relation to previously discussed frequency-dependent behaviour. Finally, we demonstrate how non-linear interaction factors may be applied to estimate pile-cap response based on a single free-field analysis.

2 | FINITE ELEMENT MODEL

2.1 | Elements, boundaries and solution schemes

The finite element model is constructed in OpenSees MP[31] together with the pre- and post-processing tool STKO.[32] Parallel computing is utilized for better (faster) performance. The ground is modelled as a half-space with symmetric y-plane. The soil is divided in eight layers, where each layer has a height $h_{lay} = 3$ m. The mesh is illustrated in Figure 2. The piles are modelled using Euler–Bernoulli beam elements and the soil is modelled using eight-noded hexahedral elements with a single integration point to prevent locking behaviour. The pile–soil interface has been considered to be an important aspect for both static and dynamic impedance of pile groups. However, recent studies[33–35] have shown that separation effects are of less significance when plasticity is considered. Also, this study only assesses the kinematic response. The interface between beams and solids is therefore modelled using rigid-link constraints (full bonding), connecting each beam node to the corresponding soil nodes such that the pile section in the given beam node acts like a rigid disk. The constraints are enforced using penalty functions[36,37] and the penalty values are obtained by approximating the order of the largest entry of the stiffness matrix.

Issues related to spurious damping are avoided by choosing a sufficiently refined element mesh. The maximum element size in each layer is determined from the shortest occurring wavelength. Shear and pressure wave velocities are determined using initial strain properties. In order to correctly represent a wave, it is necessary to use at least eight nodes per wavelength.[38] Thus, minimum of seven elements per wavelength has been used in the direction of wave propagation.

The outer, vertical boundaries perpendicular to the loading direction are represented using tied-node conditions as first suggested by Zienkiewicz et al.[39] The side boundaries are restrained from movement perpendicular to boundary plane. The bottom nodes, representing bedrock, are restrained in the vertical direction. The base motion is applied using prescribed displacements. Although the analyses are performed for rigid bedrock, the conclusions will be less dependent on this condition because the pile-cap displacements are compared with free-field soil displacements.

The system is solved using the TRBDF2 integrator[40] and Krylov–Newton implicit scheme.[41] In order to increase the probabilty of convergence and also to speed up the analysis, adaptive time steps are applied. The initial and maximum time step is 0.0025 s. If convergence is not achieved, the time step is reduced by a factor of 2. If convergence is achieved before a desired number of iterations, the time step is increased by a factor of 1.5. Since we are using penalty values as constraints, convergence is achieved when the l_2-norm of displacements is less than 1E−08 m. The chosen convergence criteria is somewhat strict due to the small displacement following from high frequency loading.

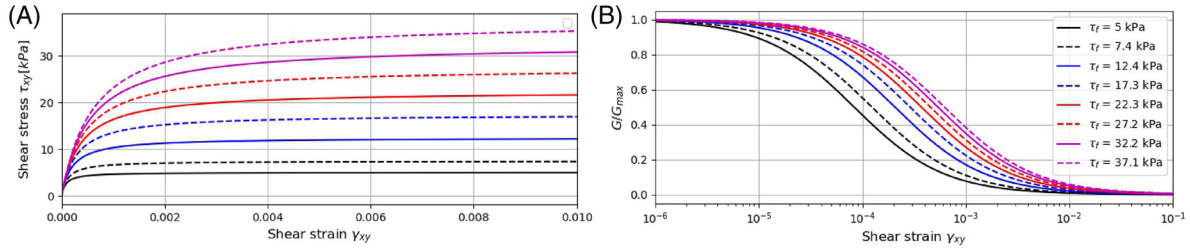

Shear stress τ_{xy} plotted against shear strain γ_{xy}.

G/G_{max} plotted against shear strain γ_{xy}.

FIGURE 3 Pressure Independent Multi-Yield (PIMY) material model

2.2 | Material model

The adopted material model (PIMY) is an elastic–plastic, soil model suited for clay.[42] Plasticity is only considered for the deviatoric stress–strain response using an associative flow rule. The input parameters are the small-strain shear modulus G_{max}, small-strain bulk modulus B_{max}, cohesion c, maximum shear strain γ_{max}, friction angle ϕ, reference confining pressure p'_r and a material parameter d controlling pressure dependence. According to Mesri,[43] the undrained shear strength of clay may be expressed as

$$\tau_f = s_u = 0.22\,\sigma'_c = 0.22\,(\gamma_s - \gamma_w)h \tag{2}$$

where σ'_c is the vertical pre-consolidation pressure, h is the soil depth and γ_s and γ_w are the specific weights of soil and water, respectively. According to Andersen,[44] small-strain shear modulus may be estimated as

$$G_{max} = G_r = 1000\,s_u \tag{3}$$

for a clay with plasticity index about 25%. The small-strain bulk modulus follows from linear elastic laws for homogeneous materials, that is

$$B_{max} = B_r = \frac{2\,G_{max}(1+\mu)}{3(1-2\mu)} \tag{4}$$

Here, μ is the Poisson's ratio set equal to 0.49. The backbone curve is determined as

$$\tau = \frac{G_{max}\,\gamma}{1 + \dfrac{\gamma}{\gamma_r}} \tag{5}$$

where

$$\gamma_r = \frac{\tau_f\,\gamma_{max}}{G_{max}\,\gamma_{max} - \tau_f} \tag{6}$$

Here, γ_{max} is the peak shear strain set equal to 0.1.

The shear stress-shear strain relations for each layer are shown in Figure 3A and the shear modulus reduction curves are shown in Figure 3B.

Maximum shear strength is shown in Figure 1. The average shear wave velocity of the profile is approximately

$$V_{s,H} = \frac{H}{\sum_{i=1}^{n_{lay}} \dfrac{h_{lay}}{V_{s,lay}}} = 91.8\frac{\text{m}}{\text{s}} \tag{7}$$

Here, n_{lay} is the total number of soil layers, h_{lay} is the layer height and $V_{s,lay}$ is the shear wave velocity of the layer.

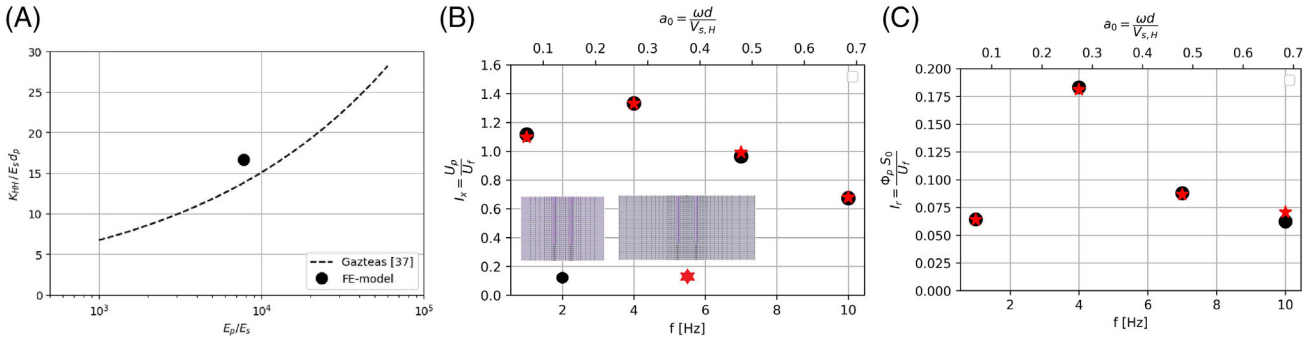

FIGURE 4 Validation of FE-model in terms of (A) static stiffness for a single pile, (B) horizontal kinematic interaction I_x and (C) rotational kinematic interaction I_r. Kinematic interaction factors in (A) and (B) are computed for a two-by one pile group ($S_0 = 6d$ and $\beta = 0^o$) and plotted against frequency f and dimensionless angular frequency a_0

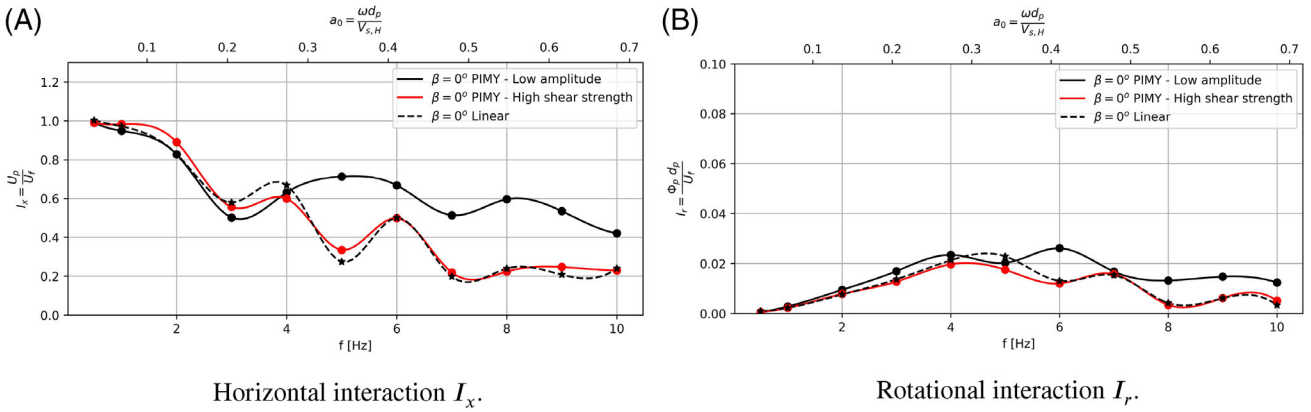

FIGURE 5 Convergence of linear and non-linear models. Kinematic interaction factors are computed for a two-by one pile group ($S_0 = 6d$ and $\beta = 0^o$) and plotted against frequency f and dimensionless angular frequency a_0

The piles are modelled using a linear material model with $E_p = 35$ GPa representative of reinforced concrete. Viscous damping with damping ratio equal to 0.02 is added to the model.

2.3 | Model verification

First, the model is compared against the solution for static stiffness of a single pile as proposed by Gazetas.[45] The closed-form expression is strictly valid for a perfect Gibson soil, but is used here only as an approximation in order to verify the FE model. The comparison is shown in Figure 4A, and the results are in reasonable agreement. The final element mesh ($\approx 27,900$ elements) and boundary conditions are verified by comparing the applied FE model against a model with larger width and finer mesh ($\approx 42,200$ elements). Interaction factors I_x and I_r are computed using the two models, and the results are shown in Figures 4B and 4C. The results match fairly well. Two additional non-linear analysis are performed, where (1) the base motion amplitude is low ($U_b = 0.001d_p$) and (2) the shear strength is set to an excessively high value. The results are shown in Figure 5. Note that we are imposing displacements at the base, which means that increasing frequency implies quadratically increasing base motion acceleration. For low base motion amplitude, it observed that the results converge in the low-frequency range. However, high shear strength yields linear response for the entire frequency range. Hence, it is concluded that the FE model is adequate for the task at hand.

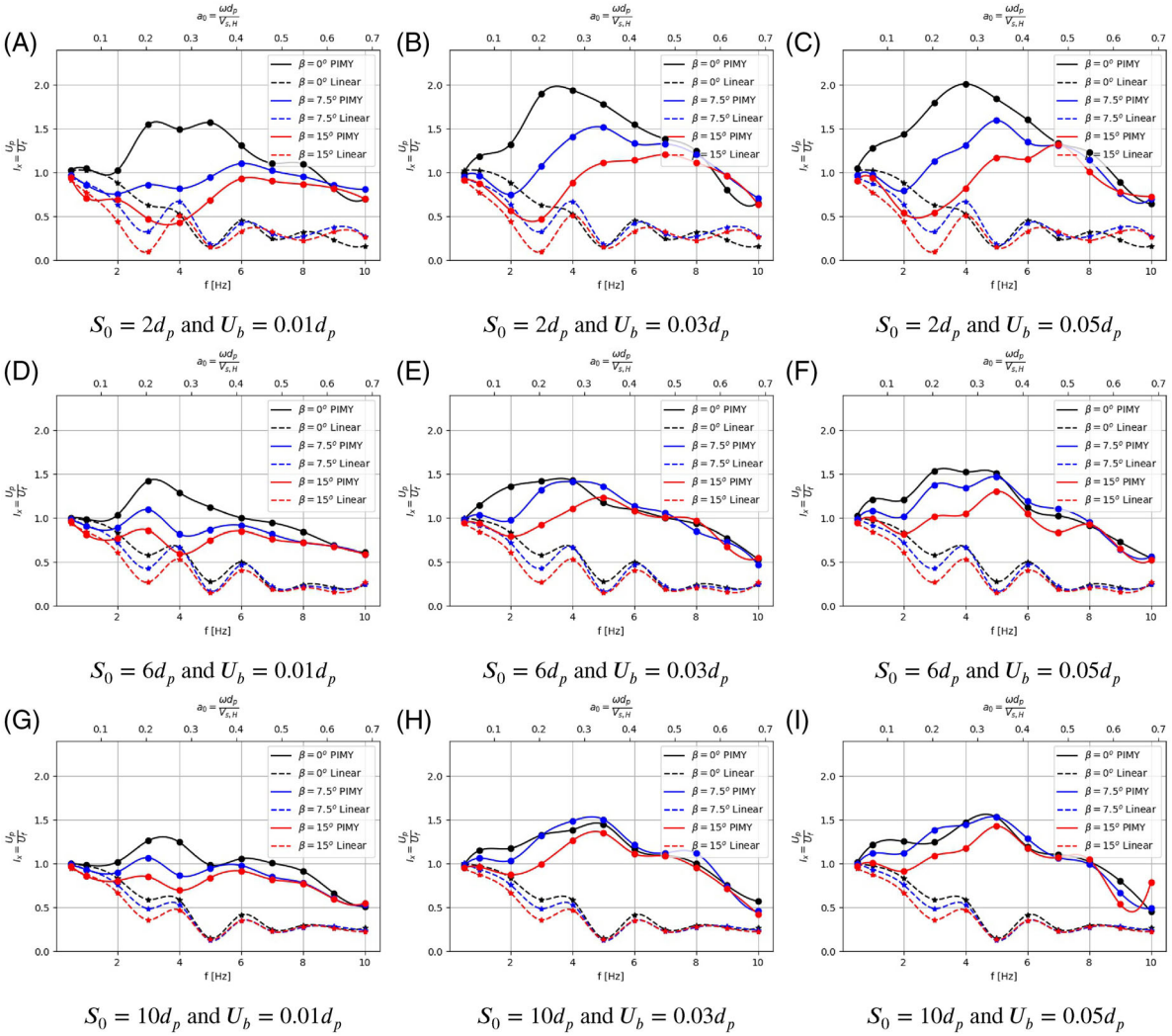

FIGURE 6 Absolute horizontal kinematic interaction factor I_x plotted against frequency f and dimensionless angular frequency a_0 for different pile-to-pile spacing S_0, batter angles β and base motion amplitudes U_b

3 | RESULTS – HARMONIC RESPONSE

3.1 | General

The results are presented in terms of horizontal and rotational interaction factors (Figures 6 and 7), normalized horizontal pile-cap displacements (Figure 8), normalized pile-cap rotations (Figure 9), normalized maximum moments (Figure 10), normalized maximum shear forces (Figure 11) and normalized maximum axial forces (Figure 12). The results are plotted against both frequency and dimensionless angular frequency, and normalization is achieved by dividing the results with the peak value in each figure. Maximum moments and forces are given independent of depth. Each plot shows three batter angle configurations ($\beta = 0°, 7.5°$ and $15°$) for a specific combination of pile-to-pile spacing ($S_0 = 2d_p, 6d_p$ and $10d_p$) and base motion amplitude ($U_B = 0.01d_p, 0.03d_p$ and $0.05d_p$). Each combination is analysed for 11 different harmonic base motion histories with frequencies between 0.5 and 10 Hz. The figures are organized such that base motion amplitude is constant column-wise and pile spacing is constant row-wise. The plots are a result of 297 non-linear and 99 linear time-history analysis in three-dimensional space. The linear analyses are performed using small-strain properties of the soil model and 5% damping. The results are plotted as functions of both frequency and dimensionless angular frequency

$$a_0 = \frac{\omega d_p}{V_{s,H}} \tag{8}$$

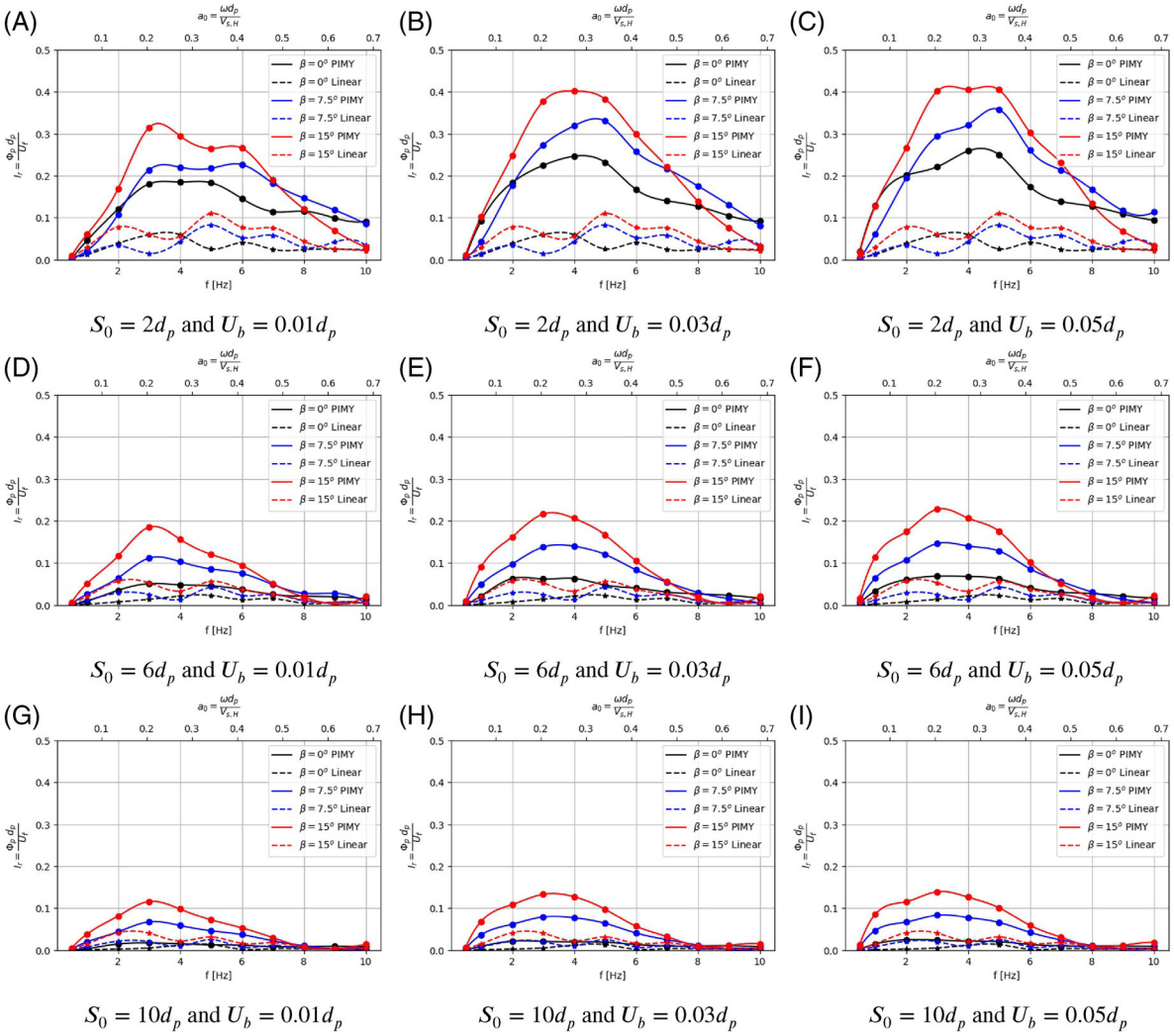

FIGURE 7 Absolute rotational kinematic interaction factor I_r plotted against frequency f and dimensionless angular frequency a_0 for different pile-to-pile spacing S_0, batter angles β and base motion amplitudes U_b

Note that we are using the approximated small-strain shear wave velocity of the soil profile to normalize the angular frequency. Otherwise, a_0 would generally not be constant in space and time, nor would it be linear with respect to angular frequency, and therefore meaningless as a plotting variable. The single-valued conversion from time to frequency domain is achieved by averaging the horizontal and rotational amplitudes during steady state response. The time domain analysis is therefore performed over a sufficiently long period in order to achieve satisfactory results.

3.2 | Kinematic interaction factor

Figure 6 shows that soil non-linearity has a substantial impact on the estimated horizontal kinematic interaction. While linear models de-amplify the horizontal ground motion for almost all configurations and frequencies, non-linear models show fairly large amplification for a wide range of frequencies. Generally, both I_x and I_r increase slightly with base motion amplitude, and the difference between $0.1d$ and $0.3d$ is more prominent compared to the difference between $0.03d$ and $0.05d$. In fact, the difference between $0.03d$ and $0.05d$ is rather negligible in most cases. This is an inherent part of the non-linear material behaviour shown in Figure 3. It also observed that base motion amplitude is most significant for small pile spacing. The largest differences between the different batter angles are observed in the low-to-mid frequency range for most configurations. As frequency increases, the difference decreases and I_x generally decreases. In the high-frequency range, I_x is practically unaffected by batter angle.

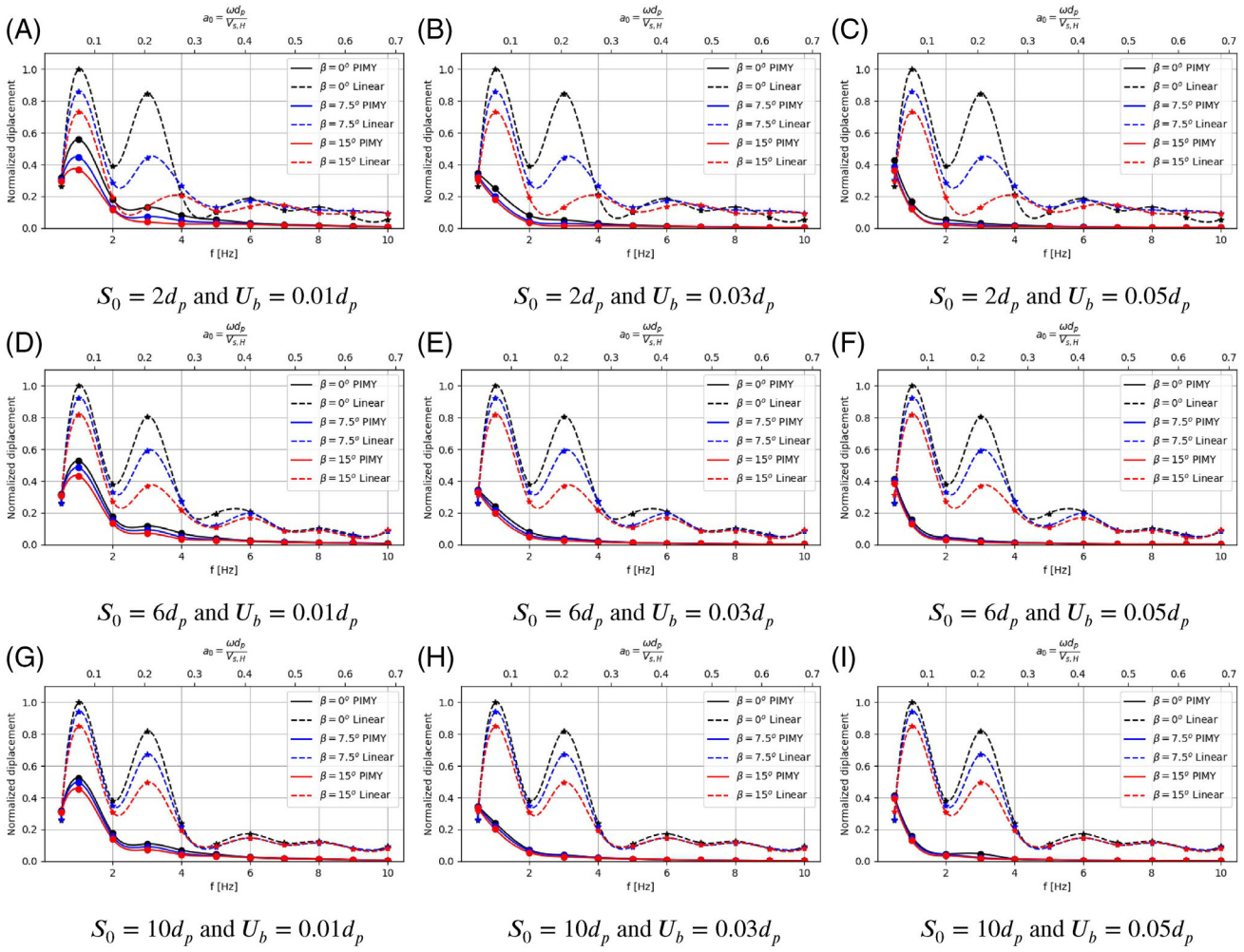

FIGURE 8 Horizontal displacement amplitude normalized by the peak value and plotted against frequency f and dimensionless angular frequency a_0 for different pile-to-pile spacing S_0, batter angles β and base motion amplitudes U_b

Eigenfrequencies of the linear soil profile may be estimated using Equation (7), that is

$$f_{H,1} = \frac{V_{s,H}}{4\mathrm{H}} = 0.96\mathrm{s}, \quad f_{H,2} = \frac{3V_{s,H}}{4\mathrm{H}} = 2.87\mathrm{s}, \quad f_{H,2} = \frac{5V_{s,H}}{4\mathrm{H}} = 4.78\mathrm{s}\ldots \tag{9}$$

Figure 6 clearly shows that horizontal interaction using linear models is most prominent near these frequencies, starting from the second eigenfrequency. For the first soil mode in the linear case, the soil response has small variations close to the surface, and the pile conforms relatively well to the soil displacements. At higher frequencies with smaller wavelengths, the pile is unable to follow the soil displacements, which leads to small I_x-values. In non-linear soil, the dramatic reduction of the soil stiffness close to the surface results in the pile's stiffness dominating the soil response leading to pile displacements larger than in the free field. Figure 7 shows that non-linearity significantly increases I_r for all configurations. Non-linear models show a clear tendency with respect to frequency, where rotation peaks at the mid-range frequencies and decays to diminishingly small values as frequency increases. Linear models, however, do not show a clear trend, but rather a steady fluctuation at relativity small values compared to the non-linear model. Linear and non-linear models seemingly tend towards convergence at higher frequencies. I_r increases with batter angle for all configurations, especially for non-linear models. Similar results were obtained in previous studies[4,23] [46,47] using linear models. There may evidently exist cut-off frequencies where increasing batter angle in fact decreases rotation, but this behaviour occurs in the high-frequency range where rotation is generally small. I_r decreases significantly as pile spacing increases for all batter angles and base motion amplitudes. Similar results were obtained by Medina et al.[23] The results also show that as pile spacing increases, batter angle becomes a more governing factor.

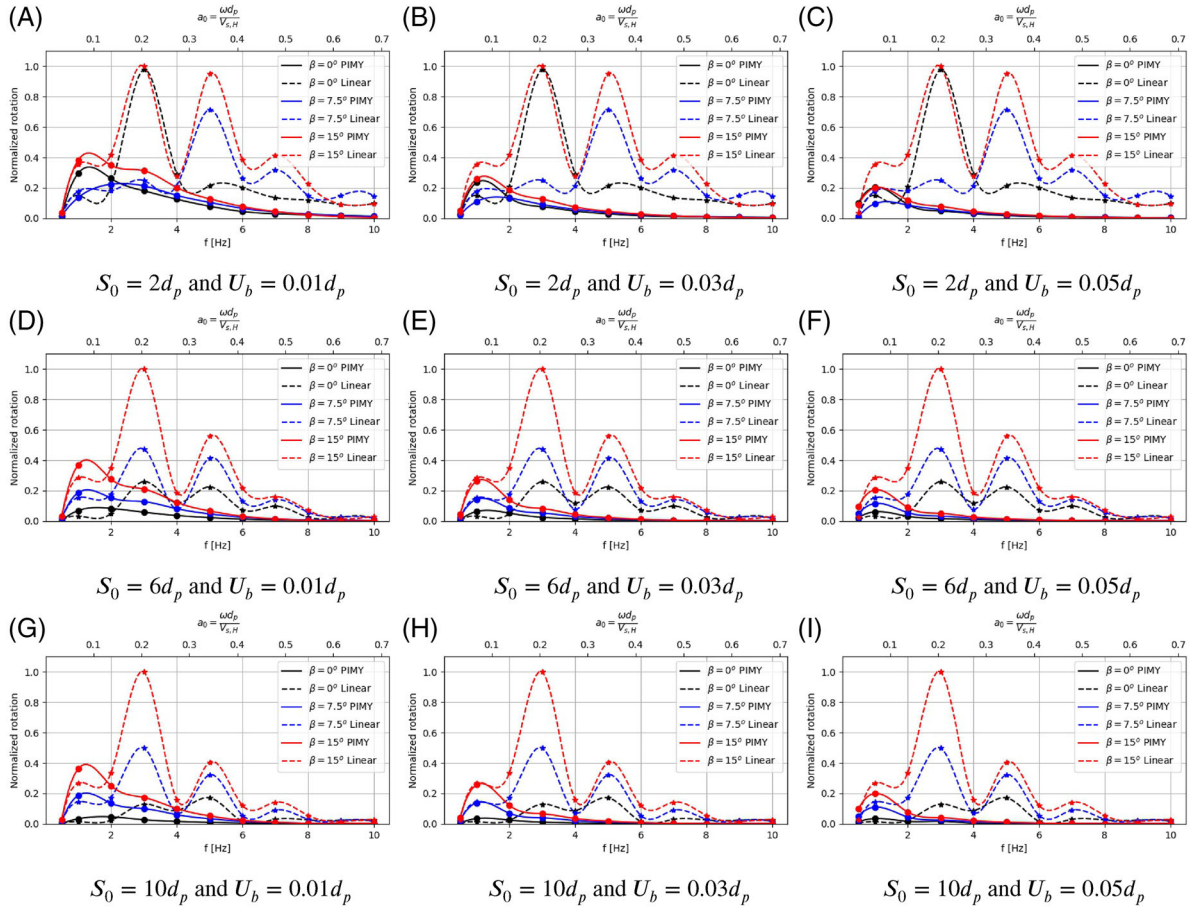

FIGURE 9 Rotation amplitude normalized by the peak value and plotted against frequency f and dimensionless angular frequency a_0 for different pile-to-pile spacing S_0, batter angles β and base motion amplitudes U_b

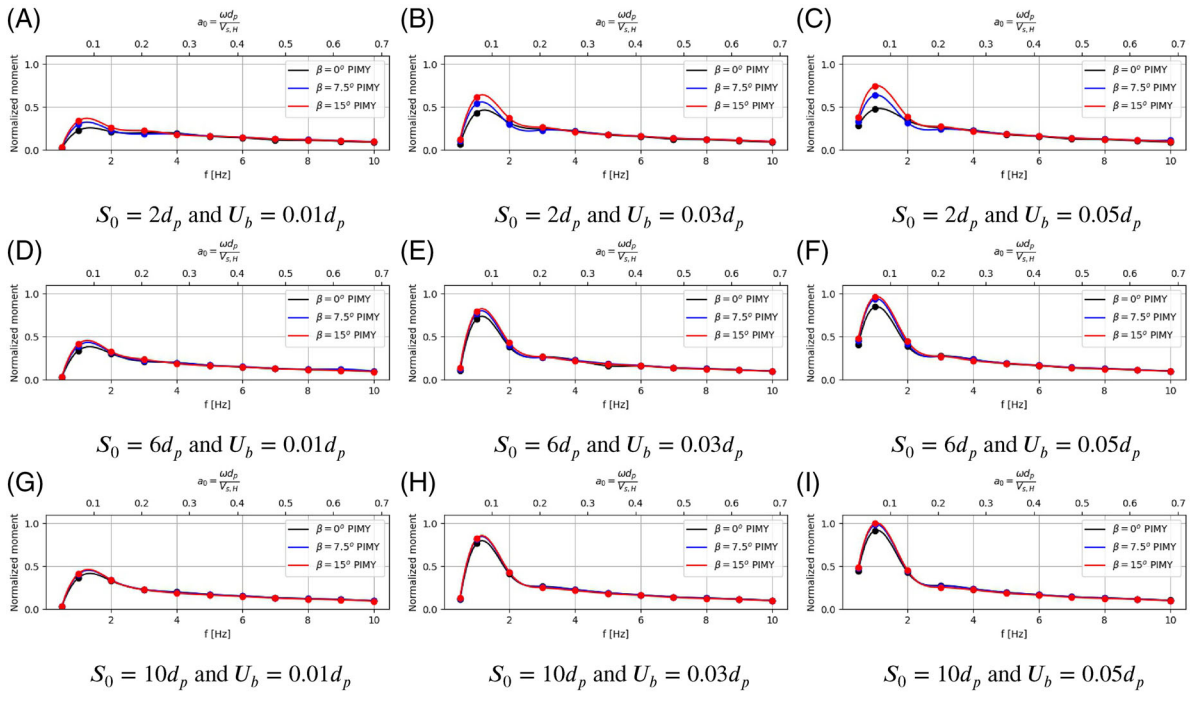

FIGURE 10 Maximum moment independent of depth normalized by the peak value and plotted against frequency f and dimensionless angular frequency a_0 for different pile-to-pile spacing S_0, batter angles β and base motion amplitudes U_b

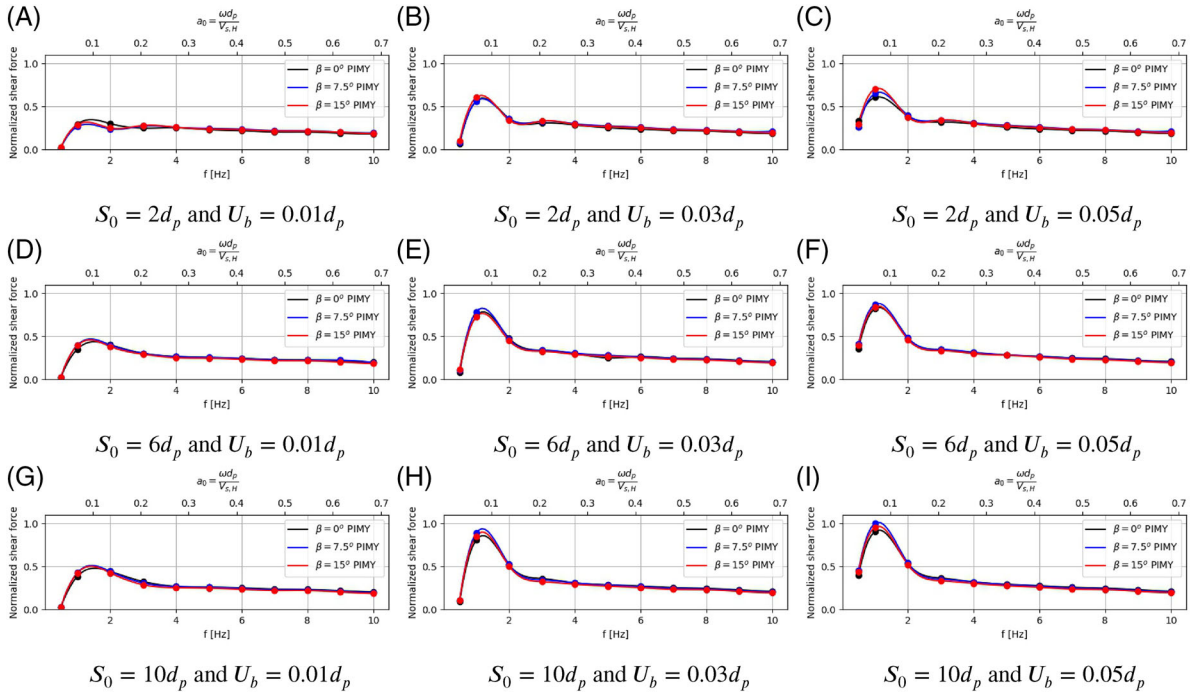

FIGURE 11 Maximum shear force independent of depth normalized by the peak value and plotted against frequency f and dimensionless angular frequency a_0 for different pile-to-pile spacing S_0, batter angles β and base motion amplitudes U_b

3.3 | Displacement and rotation amplitudes

It is important to note that the differences between linear and non-linear models shown in Figures 6 and 7 only reflect differences regarding pile–soil interaction, not differences between displacements and rotation values. In other words, these results should not be interpreted as if non-linear models produce larger pile-cap displacements and rotations. On the contrary, Figures 8 and 9 show that soil non-linearity in most cases substantially reduces displacements and rotations. As expected, Figure 8 shows that displacements peak at the first eigenfrequencies in case of linear soil. The non-linear models, however, do not exhibit this behaviour. Except for a small peak at the fundamental frequency in combination with small base motion amplitudes, displacements generally decrease as frequency increases. The peak is explained by the fact that small base motion amplitude in combination with low excitation frequency results in a more linear behaviour of the soil. Consistent with the findings regarding horizontal interaction in Figure 6, non-linearity not only reduces displacements, but also yields less frequency-dependent behaviour. Moving past the mid-to-high frequency range, non-linear models produce diminishingly small pile-cap displacements. Figure 9 reveals similar results for rotations. As was shown for rotational interaction in Figure 7, rotations decrease with increasing pile spacing for both the linear and non-linear models.

3.4 | Moments and forces

Figure 10 shows the maximum moment in a pile independent of depth normalized by the maximum moment occurring for all the cases considered (therefore, there is only one case in the figures that reaches 1.0). Results presented in Figures 8 and 9 clearly show that non-linearity reduces displacement and rotations, and it may readily be shown that same applies to moment and forces. Therefore, moments and forces will only be presented for the non-linear case. By doing so, one may observe trends with respect to base motion amplitude, batter angle and pile spacing rather clearly within the realm of non-linearity. Generally, Figure 10 shows that moments peak at the fundamental frequency and decay as frequency increases. Moments increase with batter angle, but only at or near the fundamental frequency. The difference is most prominent for small pile spacing and large shaking. Except for small differences at the fundamental frequency, moments are practically independent of batter angle for large pile spacing. It is also observed that moments tend towards small

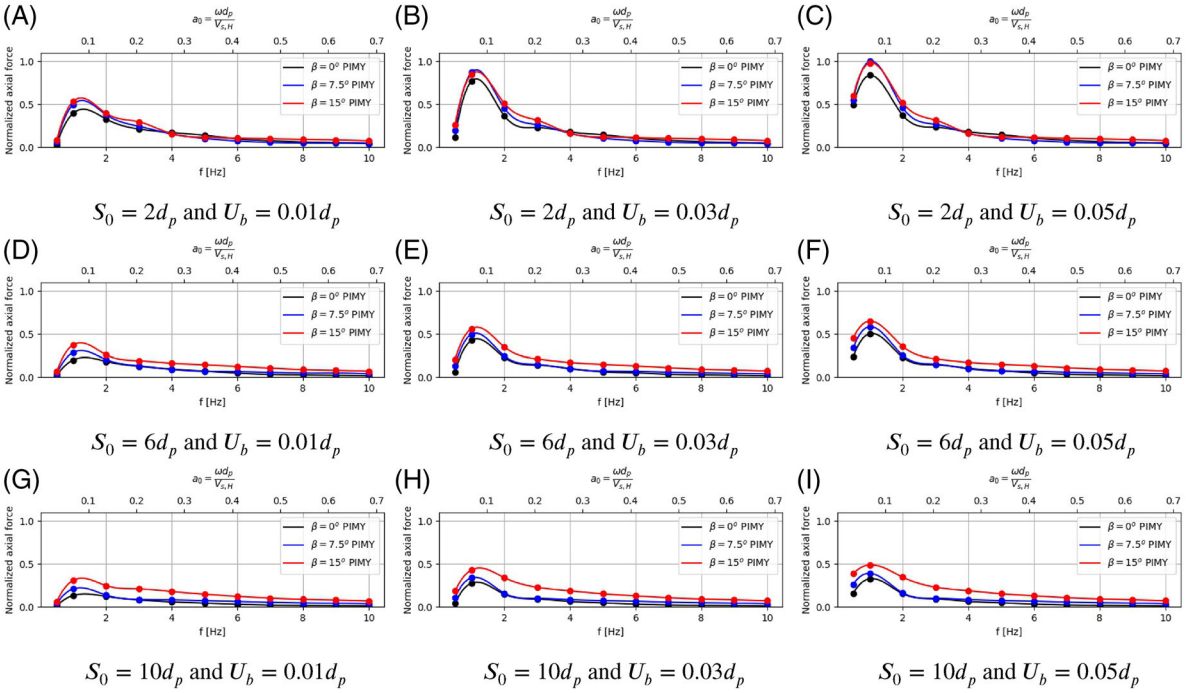

FIGURE 12 Maximum axial force independent of depth normalized by the peak value and plotted against frequency f and dimensionless angular frequency a_0 for different pile-to-pile spacing S_0, batter angles β and base motion amplitudes U_b

values in the mid-to-high frequency range for all configurations. Moments also generally increase with increasing pile spacing and shaking.

Figure 11 shows the maximum shear force in the same manner as moments. As in the case for moments, shear forces peak at the fundamental frequency, increase with pile spacing and base motion amplitude and decay as frequency increases. Shear forces also slightly increase with batter angle, but the differences are smaller compared to moments. For practical purposes, shear forces can be considered independent of batter angle.

Figures 12 shows the maximum occurring axial force in the same manner as moments and shear forces. Axial forces peak at the fundamental frequency, increase with base motion amplitude and decay as frequency increases. Contrary to moments and shear forces, axial forces decrease with increasing pile spacing. It is interesting that as pile spacing increases, the two configurations with $\beta = 0°$ and $\beta = 7.5°$ converge, while the difference compared to the configuration with $\beta = 15°$ increases. This might suggest a cut-off combination of batter angle and pile spacing, where axial forces begin to increase.

3.5 | Other practical observations

A common characteristic in the kinematic response of the two-by-one pile groups depicted in Figures 6–12, is that batter angle becomes less important as frequency increases beyond a certain value. This behaviour is attributed to the short-wavelength excitation causing reversing soil displacements over the pile length. Figure 13 shows deformation patterns at maximum pile-cap displacement for pile groups with $S_0 = 2d_p$ subjected to harmonic excitations at 3 and 8 ,Hz, respectively. These frequencies are chosen to represent the mid-to-low frequency range where large differences in kinematic interaction between batter and vertical piles begin to occur, and a high frequency range, where batter and vertical piles begin to converge. In the mid-to-low frequency range, the soil displacements are relativity uniform over the pile length, causing a large portion of piles to move somewhat uniformly in one direction. The vertical pile groups then display a rather cantilever-like deformation pattern as is shown in Figure 13A. When the pile-cap moves to the right, it rotates clockwise. The maximum displacement and rotation are in phase, and the axial pair of forces is working in the opposite direction of rotation. The batter pile group on the other hand shows a completely different deformation pattern for the same base excitation as clearly illustrated in Figure 13C. When the pile-cap moves to the right, it rotates counter clockwise. It can be

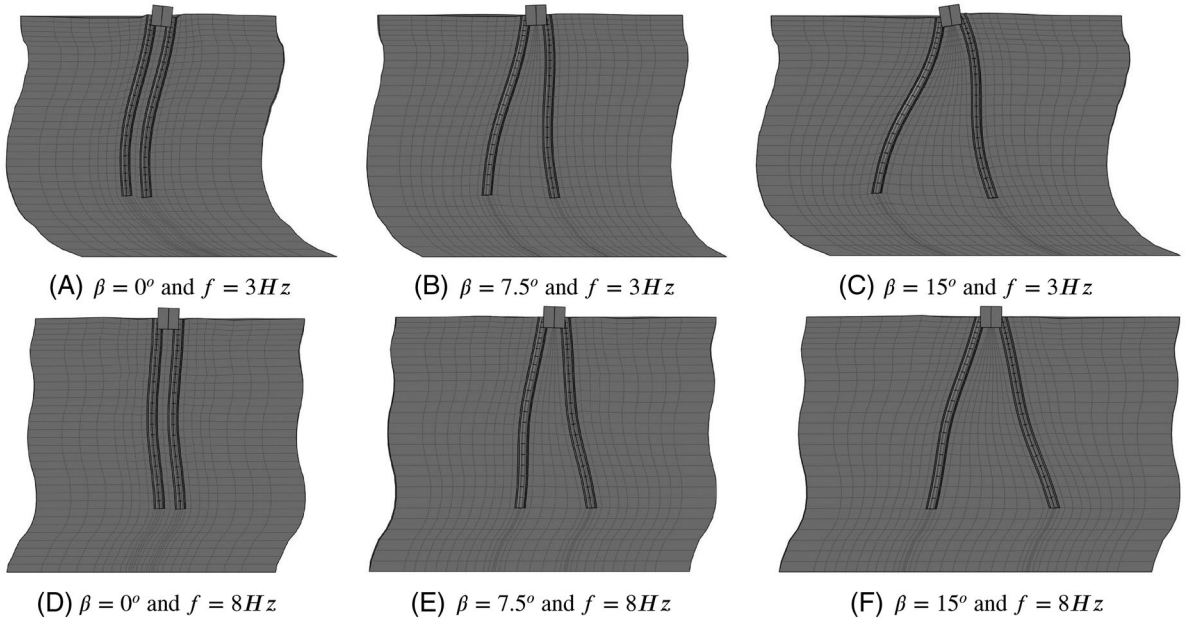

FIGURE 13 Comparison of deformed shape for various batter angles and excitation frequencies. $S_0 = 2d$ and $U_b = 0.03d$

shown that the maximum displacement and rotation are in fact out of phase, and that the axial pair of forces is working in the direction of rotation. This observation is consistent with the findings of Giannakou et al.,[4] who also reported out-of-phase displacement and rotations for batter pile groups. This indicates that increased pile-cap rotation of batter piles groups is not solely caused by increased axial force magnitude, but also by the direction in which they act. This observation is supported by the results presented in Figures 7B and 12B, which show large differences in rotation between the different batter angles at the mid-to low frequency range, but relatively small differences in axial force.

Contrary to low-frequency excitation, high frequencies cause soil displacements that reverse multiple times over the pile length, which in turn produce smaller net displacement and rotation, and thus also more similar behaviour for vertical and batter pile groups. This deformation pattern is depicted in Figure 13D–F, which further illustrates why (1) I_x and I_r tend to insignificant values as frequency increases, and (2) that shear forces are relatively larger in the high frequency range compared to moments and axial forces as can be seen in Figures 10–12.

Another common characteristic is that moments and forces imposed by kinematic interaction of pile groups are not grossly increased by batter angle, while pile-cap displacements are significantly reduced with increasing batter angle, especially for smaller pile spacing. Since inertial forces from the superstructure are governed by the magnitude of pile-cap displacements and rotations, there is reason to suspect that batter piles may be beneficial to the overall response.

4 | RESULTS – TRANSIENT RESPONSE

The results presented in the previous sections are frequency-dependent values obtained from non-linear analyses with imposed harmonic base motions. In this section, we explore how the frequency-dependent findings may relate to the system response when subjected to real earthquake time histories. In order to investigate this, four different pile groups using the largest and smallest values of S_0 and β are subjected to the horizontal component of the 1979 Imperial Valley-06 earthquake ($M = 6.4, PGA = 0.15$ g, dominant period $T_p \approx 0.1 - 1.0$ s). The results are presented as normalized horizontal and angular acceleration of the pile-cap in both time and frequency domain, in addition to normalized moments, shear forces and axial forces in the piles.

Figure 14A–D shows the horizontal and angular acceleration of the pile-cap for a group with $S_0 = 2d_p$. The results reveal that increasing batter angle decreases horizontal acceleration but increases angular acceleration. Further, the largest differences of displacements are observed in the low-to-mid frequency range, while the largest differences in angular accelerations are observed in the mid-range frequencies. These observations are in line with the frequency-dependent interaction factors presented in Figures 6 and 7. Figure 14E–H show the same results, but for a group with $S_0 = 10d_p$. As

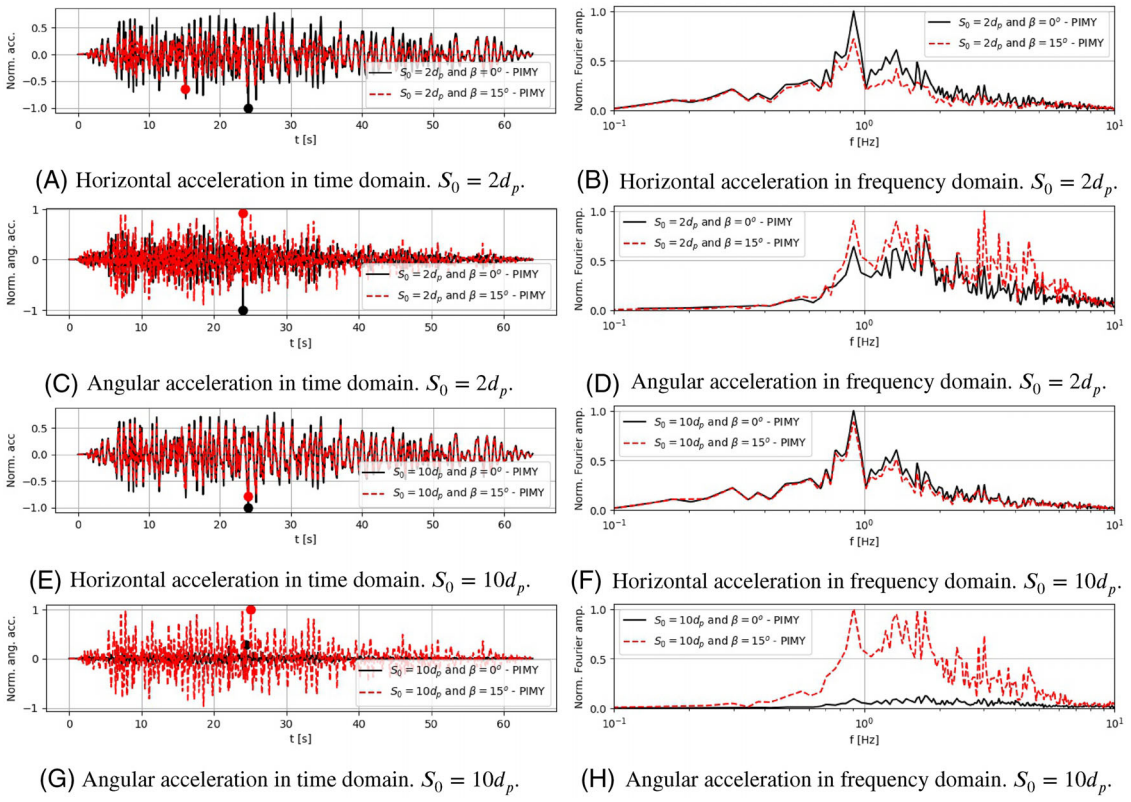

(A) Horizontal acceleration in time domain. $S_0 = 2d_p$.
(B) Horizontal acceleration in frequency domain. $S_0 = 2d_p$.
(C) Angular acceleration in time domain. $S_0 = 2d_p$.
(D) Angular acceleration in frequency domain. $S_0 = 2d_p$.
(E) Horizontal acceleration in time domain. $S_0 = 10d_p$.
(F) Horizontal acceleration in frequency domain. $S_0 = 10d_p$.
(G) Angular acceleration in time domain. $S_0 = 10d_p$.
(H) Angular acceleration in frequency domain. $S_0 = 10d_p$.

FIGURE 14 Soil profile subjected to earthquake motion. Comparison of batter angle

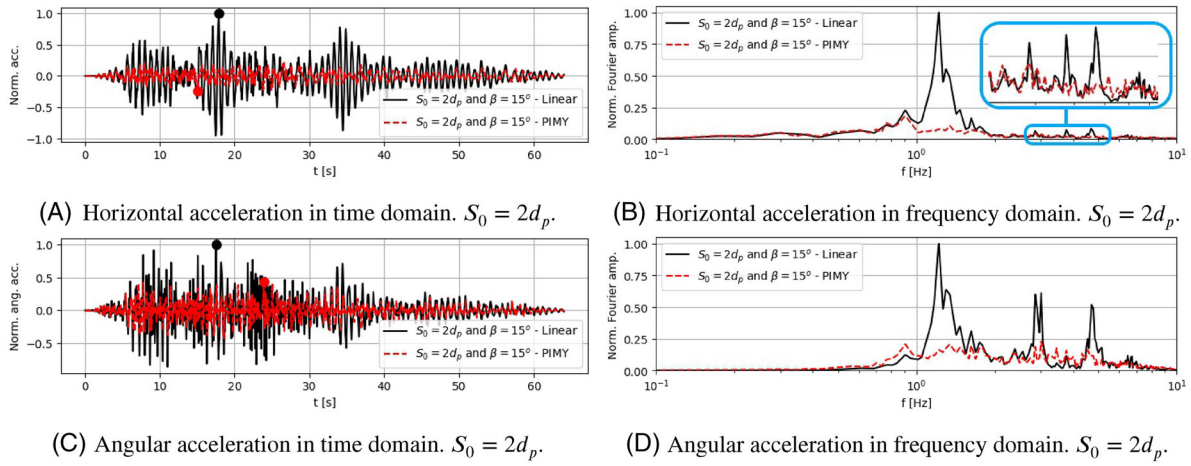

(A) Horizontal acceleration in time domain. $S_0 = 2d_p$.
(B) Horizontal acceleration in frequency domain. $S_0 = 2d_p$.
(C) Angular acceleration in time domain. $S_0 = 2d_p$.
(D) Angular acceleration in frequency domain. $S_0 = 2d_p$.

FIGURE 15 Soil profile subjected to earthquake motion. Comparison of linear against non-linear model

for close pile spacing, increasing batter angle decreases horizontal displacements and increases rotations. However, two distinctions are observed; (1) there is less difference in horizontal acceleration between the two batter angles and (2) the difference in angular rotation is substantially increased. These observations are also in line with the frequency-dependent interaction factors presented in Figures 6 and 7.

Figure 15 compares the linear model against the non-linear model. The linear model yields large peaks near the estimated eigenfrequencies of the soil profile and generally produces larger displacements and rotations, as was also demonstrated in Figures 8 and 9.

Figures 16 and 17 show the horizontal and angular acceleration of the pile-cap subjected to scaled values of the 1979 Imperial Valley-06 earthquake. It is observed that the relative behaviour of vertical and batter pile groups is not heavily influenced by the input motion PGA once the system is in the non-linear domain.

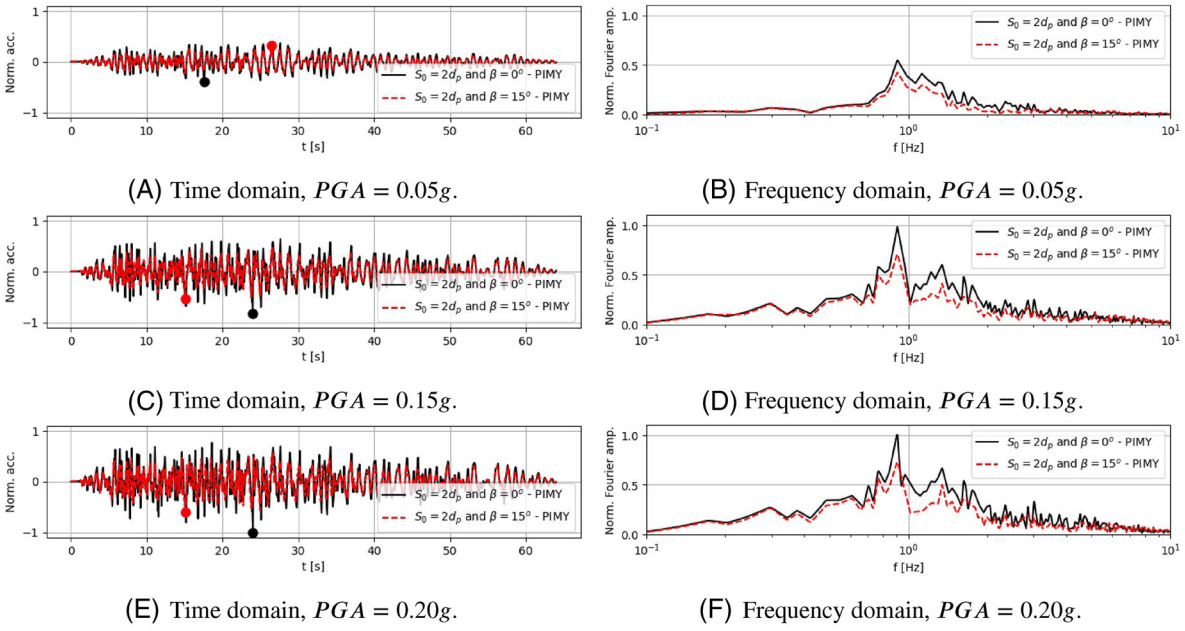

(A) Time domain, $PGA = 0.05g$. (B) Frequency domain, $PGA = 0.05g$.

(C) Time domain, $PGA = 0.15g$. (D) Frequency domain, $PGA = 0.15g$.

(E) Time domain, $PGA = 0.20g$. (F) Frequency domain, $PGA = 0.20g$.

FIGURE 16 Horizontal acceleration of the pile-cap. Comparing response for different input motion PGA. $S_0 = 2d_p$

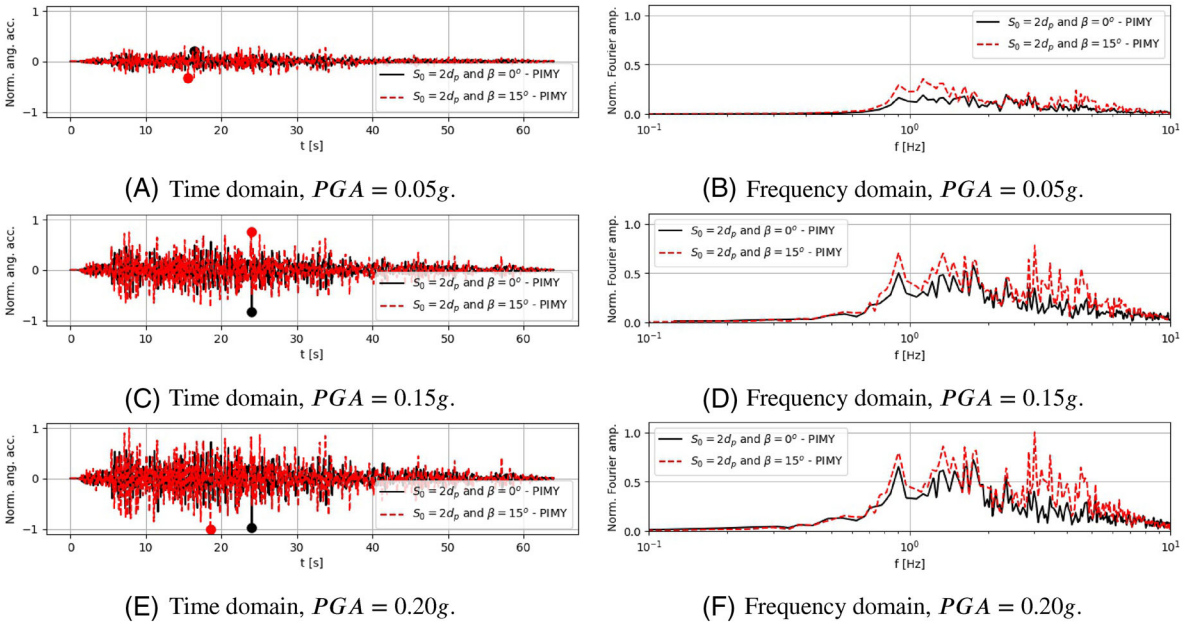

(A) Time domain, $PGA = 0.05g$. (B) Frequency domain, $PGA = 0.05g$.

(C) Time domain, $PGA = 0.15g$. (D) Frequency domain, $PGA = 0.15g$.

(E) Time domain, $PGA = 0.20g$. (F) Frequency domain, $PGA = 0.20g$.

FIGURE 17 Angular acceleration of the pile-cap. Comparing response for different input motion PGA. $S_0 = 2d_p$

Figure 18 shows the response spectrum of scaled the input motions and the resulting horizontal pile-cap motion for vertical and batter pile group with $S_0 = 2d_p$. The figures on the left hand side show the normalized response spectra for each case. The figures on the right hand side show the response spectrum of the horizontal pile-cap motion divided by the spectrum of the input motion, which is here referred to as response spectrum ratio. For low PGA, the system behaves practically linearly and the spectral accelerations are greatly amplified for both pile groups. The peak is observed near the estimated fundamental period of the soil profile. As PGA increases, the pile-cap amplification diminishes. For low periods, the spectral accelerations are in fact reduced, particularly for batter pile groups. As was also observed in Figure 16, the relative behaviour of vertical and batter pile groups is not dependent on input motion PGA when the pile–spoil system is responding well in the non-linear range. Batter pile groups generally yield lower spectral accelerations, and the difference between vertical and batter pile groups seems to be almost independent of period.

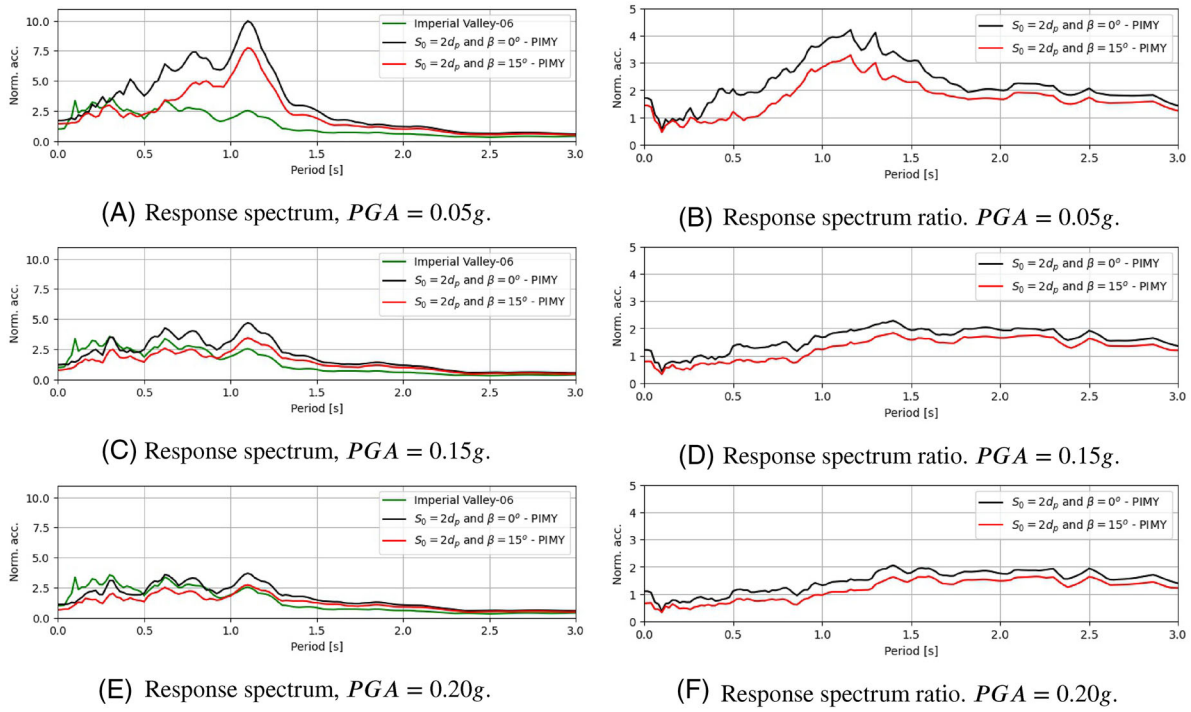

FIGURE 18 Response spectrum with 5% damping. Comparing input motion and pile-cap response for different input motion *PGA*

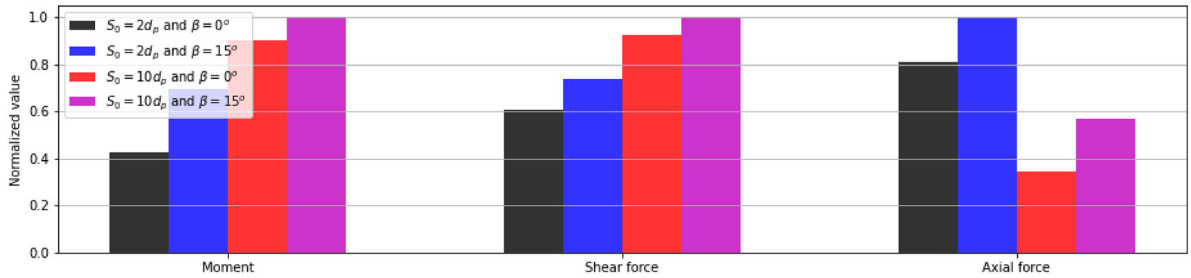

FIGURE 19 Normalized maximum forces

Figure 19 shows the maximum moment, shear force and axial force in a pile independent of depth normalized by the peak value computed in all four configurations. First, we observe that both moment and shear force increase with both pile spacing and batter angle. Second, the axial force increases with batter angle, but substantially decreases with pile spacing. Both observation are in line with the frequency-dependent results shown in Figures 10–12.

The above results indicate that the frequency-dependent results presented in Section 3 may indeed provide insight into how deep foundations respond to seismic loading and could be used to guide arrangements of the piles.

If soil–structure interaction effects are to be considered, an important part of the analysis is the assessment of foundation input motion (FIM), usually given as kinematic pile-cap response in one node. In practice, there is often a need to experiment with different batter angles and pile spacings in order to achieve satisfactory results for both foundation and superstructure. Utilizing kinematic interaction factors is quite efficient. This method implies a single computation of the free-field where the pile-cap response may readily be obtained for various pile spacings and batter angles. The superposition principle strictly restricts the method to linear soil. However, the results obtained in Section 4 together with the fact that kinematic interaction factors tend to be less dependent of base motion amplitude (*PGA*) well in the non-linear range, seems at least to provide some optimism with respect to applying the kinematic interaction factors in a traditional sense as a means for estimating the pile-cap response. An attempt is made in the following to examine how non-linear kinematic interactions can provide an estimate of the pile-cap response using both vertical and batter piles.

Figure 20 shows the estimated horizontal and angular acceleration of the pile-cap using non-linear interaction factors compared against the FE-solution. The results are normalized by the peak value in each plot. The plots on the left-hand side

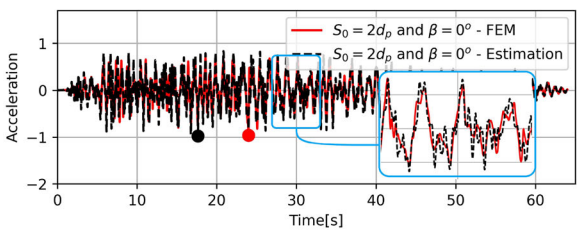

(A) Horizontal acceleration in time domain. $\beta = 0^o$.

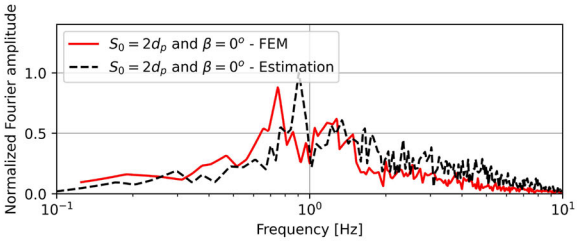

(B) Horizontal acceleration in frequency domain. $\beta = 0^o$.

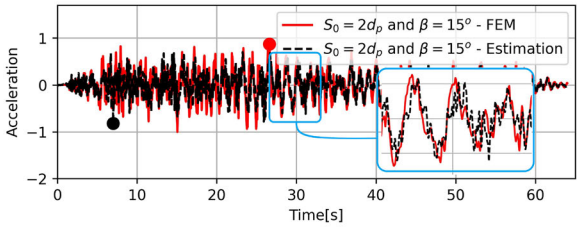

(C) Horizontal acceleration in time domain. $\beta = 15^o$.

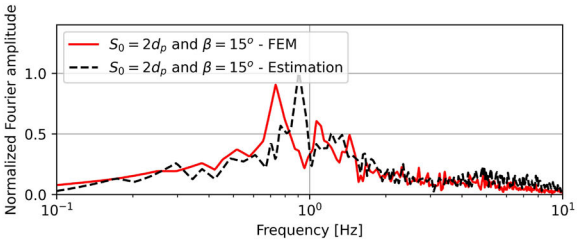

(D) Horizontal acceleration in frequency domain. $\beta = 15^o$.

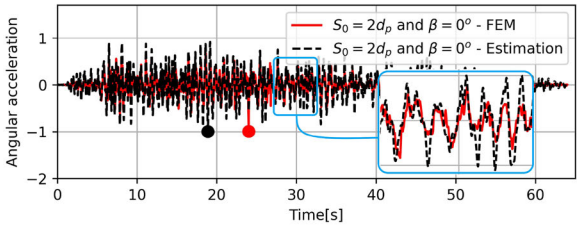

(E) Angular acceleration in time domain. $\beta = 0^o$.

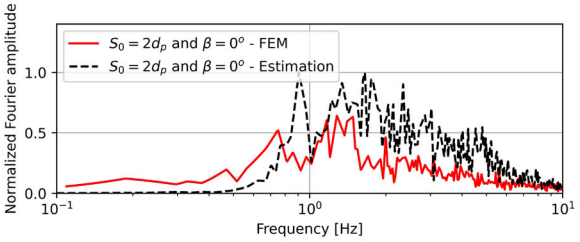

(F) Angular acceleration in frequency domain. $\beta = 0^o$.

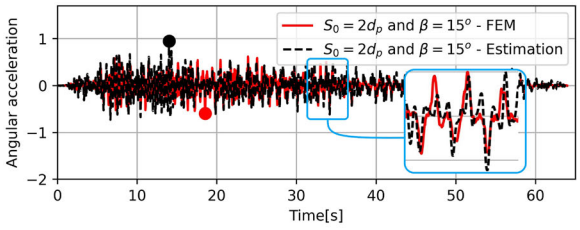

(G) Angular acceleration in time domain. $\beta = 15^o$.

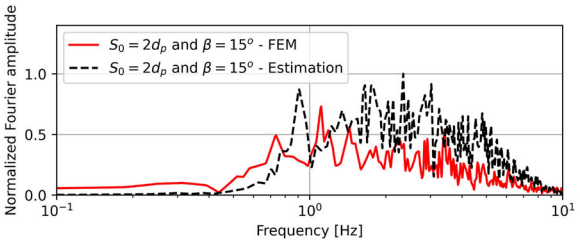

(H) Angular acceleration in frequency domain. $\beta = 15^o$.

FIGURE 20 Soil profile subjected to earthquake motion. Comparison of estimated solution against FEM-model. $S_0 = 2d_p$

show response in time domain, while the plots on right-hand side show the response in frequency domain. Figure 20A,B shows that the horizontal acceleration is generally somewhat overestimated for vertical piles, but that the trends with respect to frequency are captured fairly well. Figure 20C,D indicates similar results for batter piles. Figure 20E,F shows that angular acceleration of the pile-cap for vertical piles is overestimated to a greater degree compared to horizontal acceleration. Figure 20G,H shows similar results for batter piles. Figure 21 compares the estimated horizontal and angular acceleration for vertical and batter pile groups. The result shows that batter piles yield lower horizontal accelerations and higher angular accelerations.

These results demonstrate that although the method overestimates the response, it is evidently able to roughly capture the effects with respect to batter angle and frequency. Perhaps most importantly, the method is able to produce a rotational time-history, which is not explicitly available from free-field site response analyses. Since base motion amplitude (*PGA*) does not affect the kinematic interaction factors, the utilized interaction factors were taken from Figures 6B and 7B for these analyses. Note that the kinematic interaction factors presented in Figures 6 and 7 are given in absolute form, and are therefore lacking information about phase differences between free-field and pile-cap response. However, the interaction factors applied in the estimation are in fact complex numbers containing information about the phase. The blown-up time-histories in Figure 20 show that phase shifts are roughly captured for the most important frequencies.

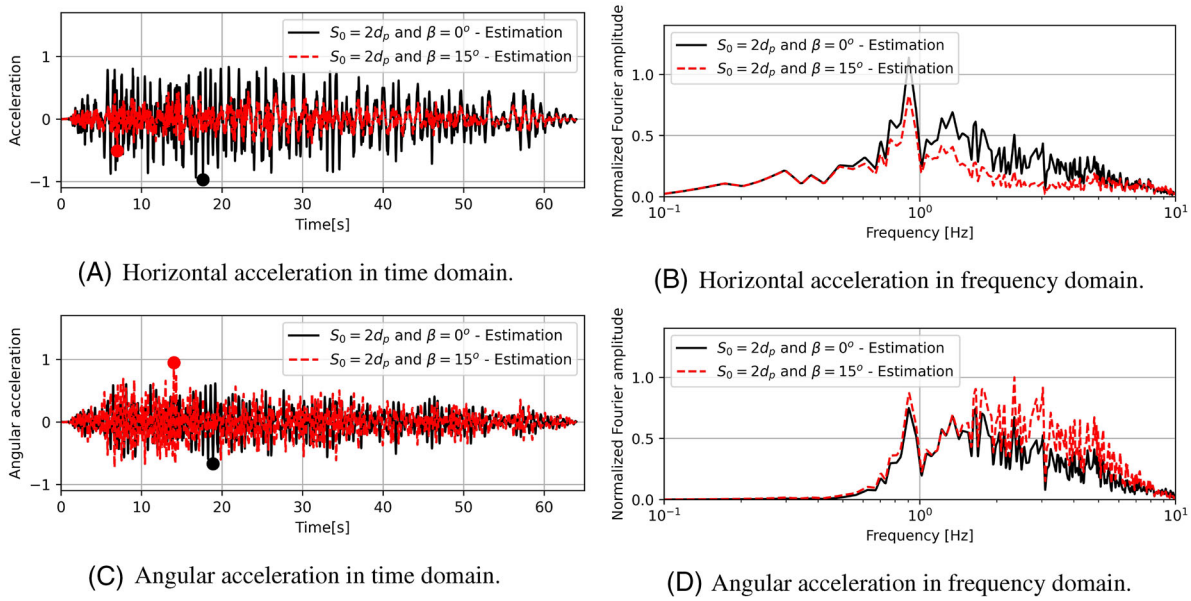

(A) Horizontal acceleration in time domain.

(B) Horizontal acceleration in frequency domain.

(C) Angular acceleration in time domain.

(D) Angular acceleration in frequency domain.

FIGURE 21 Soil profile subjected to earthquake motion. Comparison of batter angle using estimated solution. $S_0 = 2d_p$

These results strengthen the earlier observation that the non-linear kinematic interaction factors can be suitable in a preliminary design stage or as a means of investigating the effects of batter angle and pile spacing rather than producing accurate results.

5 | CONCLUSIONS

1. Soil non-linearity has a profound impact on the horizontal kinematic interaction, where non-linear models may amplify the ground motion for a wide range of configurations and frequencies. Soil non-linearity significantly increases rotational kinematic interaction for all considered configurations. However, non-linearity in most cases substantially reduces displacements and rotations amplitudes.
2. Soil non-linearity produces less frequency-dependent results.
3. Increasing batter angle decreases horizontal displacements and increases pile-cap rotations. The largest differences in kinematic interaction between the different batter angles is observed in the low-to-mid frequency range for most configurations. Moments, shear forces and normal forces generally increase with batter angle.
4. Increasing pile spacing decreases pile-cap rotation, while batter angle simultaneously becomes a more governing factor. Moments and shear forces increase with increasing pile spacing, while axial forces simultaneously decrease.
5. Increasing base motion amplitude does not significantly affect the kinematic interaction factors, but generally increases displacements, rotations, moments, shear forces and axial forces.
6. Pile-cap displacements, rotations, pile moments, shear forces and axial forces generally decrease with increasing frequency, primarily driven by the short-wavelength excitation causing reversing soil displacements over the pile length. Batter angle becomes less important as frequency increases.
7. Different deformation patterns occur for vertical and batter pile groups. Pile-cap displacements and rotations are in phase for vertical pile groups and out of phase for batter pile groups, which indicates that the increased pile-cap rotation of batter pile groups is not solely caused by increased axial force magnitude, but also by the direction in which they act.
8. For input motions with high PGA, the spectral accelerations of the pile-cap may be lower compared to the spectral acceleration of the input motion.
9. Batter pile groups generally yield lower spectral accelerations, and the difference between vertical and batter pile groups seems to be almost independent of period.
10. Estimation using non-linear kinematic interaction factors conservatively estimates the pile-cap displacements and rotations, while roughly captures the effects with respect to batter angle and frequency content.

ACKNOWLEDGMENTS

The first author would like to express gratitude to Sweco Norway AS and The Research Council of Norway for financial support.

CONFLICT OF INTEREST

The authors declare no potential conflict of interests.

DATA AVAILABILITY STATEMENT

Data sharing not applicable to this article as no datasets were generated or analysed during the current study.

ORCID

Miran Cemalovic https://orcid.org/0000-0002-0639-1909
Jan B. Husebø https://orcid.org/0000-0003-3575-4745
Amir M. Kaynia https://orcid.org/0000-0002-7774-3860

REFERENCES

1. Normalisation dCE. Eurocode 8: design of structures for earthquake resistance: part 1: general rules, seismic actions and rules for buildings. European Committee for Standardization; 2004.
2. Sadek M, Isam S. Three-dimensional finite element analysis of the seismic behavior of inclined micropiles. *Int J Soil Dyn Earthq Eng*. 2004;24(6):473-485.
3. Gerolymos N, Giannakou A, Anastasopoulos I, Gazetas G. Evidence of beneficial role of inclined piles: observations and summary of numerical analyses. *Bull Earthq Eng*. 2008;6(4):705-722.
4. Giannakou A, Gerolymos N, Gazetas G, Tazoh T, Anastasopoulos I. Seismic behavior of batter piles: elastic response. *J Geotech Geoenviron Eng*. 2010;136(9):1187-1199.
5. Medina C, Padrón LA, Aznárez JJ, Maeso O. Influence of pile inclination angle on the dynamic properties and seismic response of piled structures. *Soil Dyn Earthq Eng*. 2015;69:196-206.
6. Carbonari S, Morici M, Dezi F, Gara F, Leoni G. Soil-structure interaction effects in single bridge piers founded on inclined pile groups. *Int J Soil Dyn Earthq Eng*. 2017;92:52-67.
7. Escoffier S. Experimental study of the effect of inclined pile on the seismic behavior of pile group. *Int J Soil Dyn Earthq Eng*. 2012;42:275-291.
8. Subramanian R, Boominathan A. Dynamic experimental studies on lateral behaviour of batter piles in soft clay. *Int J Geotech Eng*. 2016;10(4):317-327.
9. Bharathi M, Dubey R, Shukla SK. Experimental investigation of vertical and batter pile groups subjected to dynamic loads. *Int J Soil Dyn Earthq Eng*. 2019;116:107-119.
10. Kaynia AM. Dynamic Stiffnesses and Seismic Response of Pile Groups. *Research Report R82-03*. Department of Civil Engineering, MIT; 1982.
11. Kaynia AM, Kausel E. Dynamics of piles and pile groups in layered soil media. *Int J Soil Dyn Earthq Eng*. 1991;10(8):386-401.
12. Fan K, Gazetas G, Kaynia A, Kausel E, Ahmad S. Kinematic seismic response of single piles and pile groups. *J Geotech Eng*. 1991;117(12):1860-1879.
13. Gazetas G. Seismic response of end-bearing single piles. *Int J Soil Dyn Earthq Eng*. 1984;3(2):82-93.
14. Makris N, Gazetas G. Dynamic pile–soil–pile interaction. Part II: lateral and seismic response. *Earthq Eng Struct Dyn*. 1992;21(2):145-162.
15. Makris N. Soil–pile interaction during the passage of Rayleigh waves: an analytical solution. *Earthq Eng Struct Dyn*. 1994;23(2):153-167.
16. Gazetas G, Fan K, Kaynia A. Dynamic response of pile groups with different configurations. *Int J Soil Dyn Earthq Eng*. 1993;12(4):239-257.
17. Kavvads M, Gazetas G. Kinematic seismic response and bending of free-head piles in layered soil. *Geotechnique*. 1993;43(2):207-222.
18. Mylonakis G, Gazetas G. Kinematic pile response to vertical P-wave seismic excitation. *J Geotech Geoenviron Eng*. 2002;128(10):860-867.
19. Dezi F, Carbonari S, Leoni G. A model for the 3D kinematic interaction analysis of pile groups in layered soils. *Earthq Eng Struct Dyn*. 2009;38(11):1281-1305.
20. Kaynia AM. Dynamic response of pile foundations with flexible slabs. *Earthq Struct*. 2012;3(3-4):495-506.
21. Anoyatis G, Di Laora R, Mandolini A, Mylonakis G. Kinematic response of single piles for different boundary conditions: analytical solutions and normalization schemes. *Int J Soil Dyn Earthq Eng*. 2013;44:183-195.
22. Alamo GM, Aznárez JJ, Padrón LA, Martinez-Castro AE, Maeso O. Importance of using accurate soil profiles for the estimation of pile kinematic input factors. *J Geotech Geoenviron Eng*. 2019;145(8):04019035.
23. Medina C, Padrón LA, Aznárez JJ, Santana A, Maeso O. Kinematic interaction factors of deep foundations with inclined piles. *Earthq Eng Struct Dyn*. 2014;43(13):2035-2050.
24. Dezi F, Carbonari S, Morici M. A numerical model for the dynamic analysis of inclined pile groups. *Earthq Eng Struct Dyn*. 2016;45(1):45-68.
25. Carbonari S, Morici M, Dezi F, Leoni G. Analytical evaluation of impedances and kinematic response of inclined piles. *Eng Struct*. 2016;117:384-396.
26. Badoni D, Makris N. Nonlinear response of single piles under lateral inertial and seismic loads. *Int J Soil Dyn Earthq Eng*. 1996;15(1):29-43.

27. Hussien MN, Karray M, Tobita T, Iai S. Kinematic and inertial forces in pile foundations under seismic loading. *Comput Geotech*. 2015;69:166-181.
28. Brandenberg S, Turner B, Stewart J. *Influence of Kinematic SSI on Foundation Input Motions for Pile-supported Bridges*. 2017.
29. Wang Y, Orense RP. Numerical analysis of seismic performance of inclined piles in liquefiable sands. *Int J Soil Dyn Earthq Eng*. 2020;139:106274.
30. Rajeswari J, Sarkar R. A three-dimensional investigation on performance of batter pile groups in laterally spreading ground. *Int J Soil Dyn Earthq Eng*. 2021;141:106508.
31. UC Berkeley. OpenSees v3.2.2. Open source finite element code. 2021.
32. ASDEA Software. STKO 2021 v.2.0.5. Pre- and postprocessing tool kit for OpenSees. 2020.
33. Sarkar R, Maheshwari B. Effects of separation on the behavior of soil–pile interaction in liquefiable soils. *Int J Geomech*. 2012;12(1):1-13.
34. Rahmani A, Pak A. Dynamic behavior of pile foundations under cyclic loading in liquefiable soils. *Comput Geotech*. 2012;40:114-126.
35. Kanellopoulos K, Gazetas G. Vertical static and dynamic pile-to-pile interaction in non-linear soil. *Géotechnique*. 2020;70(5):432-447.
36. Belytschko T, Liu WK, Moran B, Elkhodary K. *Nonlinear Finite Elements for Continua and Structures*. John Wiley & Sons; 2014.
37. Kolbein B. *Engineering Approach to Finite Element Analysis of Linear Structural Mechanics Problems*. Akademika Publishing; 2015.
38. Serón F, Sanz F, Kindelan M, Badal J. Finite-element method for elastic wave propagation. *Commun Appl Numer Methods*. 1990;6(5):359-368.
39. Zienkiewicz O, Bicanic N, Shen F. *Earthquake Input Definition and the Trasmitting Boundary Conditions*. Springer; 1989:109-138.
40. Bathe KJ. Conserving energy and momentum in nonlinear dynamics: a simple implicit time integration scheme. *Comput Struct*. 2007;85(7-8):437-445.
41. Scott MH, Fenves GL. Krylov subspace accelerated Newton algorithm: application to dynamic progressive collapse simulation of frames. *J Struct Eng*. 2010;136(5):473-480.
42. Gu Q, Conte JP, Elgamal A, Yang Z. Finite element response sensitivity analysis of multi-yield-surface J2 plasticity model by direct differentiation method. *Comput Meth Appl Mech Eng*. 2009;198(30-32):2272-2285.
43. Mesri G. New design procedure for stability of soft clays. *J Geotech Geoenviron Eng*. 1975;101:409-412.
44. Andersen KH. Cyclic soil parameters for offshore foundation design. *Proceedings of the Frontiers in Offshore Geotechnics III*. 2015:5-82.
45. Gazetas G. *Foundation Vibrations*. Springer; 1991:553-593.
46. Poulos HG. Raked piles – Virtues and drawbacks. *J Geotech Geoenviron Eng*. 2006;132(6):795-803.
47. Medina C, Aznárez JJ, Padrón LA, Maeso O. Seismic response of deep foundations and piled structures considering inclined piles. In 11th World Congress on Computational Mechanics, WCCM 2014, 5th European Conference on Computational Mechanics, ECCM 2014 and 6th European Conference on Computational Fluid Dynamics, ECFD. 2014.

How to cite this article: Cemalovic M, Husebø JB, Kaynia AM. Kinematic response of vertical and batter pile groups in non-linear soft soil. *Earthquake Engng Struct Dyn*. 2022;1–19. https://doi.org/10.1002/eqe.3662